





OPEN ACCESS

Original research

Methionine deficiency facilitates antitumour immunity by altering m⁶A methylation of immune checkpoint transcripts

Ting Li,^{1,2} Yue-Tao Tan,¹ Yan-Xing Chen,¹ Xiao-Jun Zheng,³ Wen Wang,⁴ Kun Liao,¹ Hai-Yu Mo,¹ Junzhong Lin,^{1,5} Wei Yang,⁶ Hai-Long Piao,⁴ Rui-Hua Xu ,^{1,7} Huai-Qiang Ju ^{1,7}

► Additional supplemental material is published online only. To view, please visit the journal online (<http://dx.doi.org/10.1136/gutjnl-2022-326928>).

For numbered affiliations see end of article.

Correspondence to

Professor Huai-Qiang Ju and Professor Rui-Hua Xu, Sun Yat-sen University Cancer Center, Guangzhou, Guangdong, China; juhq@sysucc.org.cn, xurh@sysucc.org.cn and Professor Hai-Long Piao, Dalian Institute of Chemical Physics, Chinese Academy of Sciences, Dalian, Liaoning, China; hpiao@dicp.ac.cn

TL, Y-TT, Y-XC and X-JZ contributed equally.

Received 7 January 2022
Accepted 14 June 2022



© Author(s) (or their employer(s)) 2022. Re-use permitted under CC BY-NC. No commercial re-use. See rights and permissions. Published by BMJ.

To cite: Li T, Tan Y-T, Chen Y-X, et al. *Gut* Epub ahead of print: [please include Day Month Year]. doi:10.1136/gutjnl-2022-326928

ABSTRACT

Objective Methionine metabolism is involved in a myriad of cellular functions, including methylation reactions and redox maintenance. Nevertheless, it remains unclear whether methionine metabolism, RNA methylation and antitumour immunity are molecularly intertwined.

Design The antitumour immunity effect of methionine-restricted diet (MRD) feeding was assessed in murine models. The mechanisms of methionine and YTH domain-containing family protein 1 (YTHDF1) in tumour immune escape were determined in vitro and in vivo. The synergistic effects of MRD or YTHDF1 depletion with PD-1 blockade were also investigated.

Results We found that dietary methionine restriction reduced tumour growth and enhanced antitumour immunity by increasing the number and cytotoxicity of tumour-infiltrating CD8⁺ T cells in different mouse models. Mechanistically, the S-adenosylmethionine derived from methionine metabolism promoted the N⁶-methyladenosine (m⁶A) methylation and translation of immune checkpoints, including PD-L1 and V-domain Ig suppressor of T cell activation (VISTA), in tumour cells. Furthermore, MRD or m⁶A-specific binding protein YTHDF1 depletion inhibited tumour growth by restoring the infiltration of CD8⁺ T cells, and synergised with PD-1 blockade for better tumour control. Clinically, YTHDF1 expression correlated with poor prognosis and immunotherapy outcomes for cancer patients.

Conclusions Methionine and YTHDF1 play a critical role in anticancer immunity through regulating the functions of T cells. Targeting methionine metabolism or YTHDF1 could be a potential new strategy for cancer immunotherapy.

INTRODUCTION

Current immune checkpoint blockade (ICB) therapies, including antibodies targeting programmed cell death protein 1 (PD-1) or programmed death-ligand 1 (PD-L1), have demonstrated unprecedented clinical efficacy in treating melanoma and other malignancies.¹ However, only 15%–20% of patients exhibit clinical responses, while the remainder do not respond because of immune evasion and therapeutic resistance.² Thus, novel combination therapies incorporating ICB and

WHAT IS ALREADY KNOWN ON THIS TOPIC

- ⇒ Methionine metabolism is involved in many cellular functions and methionine restriction blocks tumour growth.
- ⇒ RNA N⁶-methyladenosine (m⁶A) modification has been reported to participate in tumour progression and antitumour immunity in a variety of tumours.
- ⇒ Homeostasis of the immune system is controlled by immune checkpoints and tumours hijack these molecules to evade immune surveillance and therapeutic resistance.

WHAT THIS STUDY ADDS

- ⇒ Methionine plays critical roles in anticancer immunity and the functions of T cells by providing a methyl donor for RNA m⁶A modification.
- ⇒ YTHDF1 and methionine metabolism are involved in regulating the expression of immune checkpoint molecules, including PD-L1 and V-domain Ig suppressor of T cell activation (VISTA), through the epigenetic regulatory mechanisms.
- ⇒ A methionine-restricted diet or YTHDF1 depletion inhibited tumour growth and synergised with PD-1 blockade for better tumour control.
- ⇒ High YTHDF1 expression correlates with poor immunotherapy outcomes.

HOW THIS STUDY MIGHT AFFECT RESEARCH, PRACTICE OR POLICY

- ⇒ Dietary methionine interventions may shed light on new strategies for cancer immunotherapy.
- ⇒ YTHDF1 is a novel potential biomarker for immunotherapy outcomes and has the potential to distinguish patients who could derive greater benefit from immune checkpoint blockade therapies.

efficacy prediction markers are urgently needed and have been extensively investigated in preclinical and clinical studies.^{1,2} For example, our recent clinical trial showed that PD-1 blockade plus chemotherapy (paclitaxel and cisplatin) significantly improved

overall survival (OS) among patients with advanced oesophageal carcinoma.³ We also identified several positive predictive markers for ICB therapies, including microsatellite instability, tumour mutational burden and DNA polymerase epsilon mutations.^{4,5} In addition, elucidating the potential regulatory mechanisms of immune checkpoints is critical for developing effective strategies for tumour immunotherapy.

Nutrition exerts considerable effects on health, and dietary interventions are commonly used to treat metabolic disease. Increasing evidence has indicated that dietary restriction of specific essential amino acids can alter cancer development and therapeutic outcomes.^{6–8} Methionine is an essential amino acid and the most variable metabolite found in human plasma.⁹ Methionine metabolism is involved in many cellular functions, including methylation reactions, redox maintenance and folate metabolism.¹⁰ A recent study showed that additional methionine supplementation by intratumoural injection into tumour-bearing mice delayed tumour growth and observed a synergistic antitumour effect with anti-PD-L1 blockade.¹¹ However, whether dietary methionine restriction affects ICB therapeutic outcomes has not yet been investigated.

Methionine is converted to S-adenosylmethionine (SAM) catalysed by methyltransferases to yield methylated substrates, involved in histone methylation, 5-methylcytosine (5-mC) DNA methylation and N⁶-methyladenosine (m⁶A) RNA methylation.⁹ RNA m⁶A modification has been uncovered in another critical layer of the epigenetic regulation of various cellular processes. However, whether immunosuppressive molecules and ICB therapeutic outcomes are influenced by methionine metabolism and RNA m⁶A modification remains largely unknown.

In this study, we showed that methionine metabolism influenced immunotherapy responses by regulating PD-L1 and V-domain Ig suppressor of T cell activation (VISTA) expression in an m⁶A-dependent manner. We revealed a novel mechanistic connection among methionine metabolism, m⁶A methylation and antitumour immunity in tumour progression, and suggested that methionine dietary intervention or targeting m⁶A-specific binding protein YTH domain-containing family protein 1 (YTHDF1) is a potential therapeutic approach in antitumour immunotherapy.

MATERIALS AND METHODS

The details are described in online supplemental materials and methods.

RESULTS

Methionine is critical for antitumour immunity

To investigate whether restricting methionine from the diet inhibits tumour growth by activating tumour immunity, we subcutaneously inoculated CT26 cells into immunocompetent syngeneic mice (BALB/c) and immunodeficient *Rag2*^{-/-} mice and fed these mice a control diet (CD) or methionine-restricted diet (MRD), respectively. MRD feeding significantly reduced serum methionine in both mouse strains after 5 days (online supplemental figure S1A). MRD feeding inhibited tumour growth by CT26 cells and MC38 cells in both groups, but the inhibitory effect was more obvious in immunocompetent syngeneic mice (BALB/c and C57BL/6J), suggesting that MRD feeding played an antitumour role through adaptive immunity (figure 1A,B, online supplemental figure S1B,C). As previously reported, methionine restriction medium inhibited tumour cell growth and increased cell death and endogenous lactate dehydrogenase release (online supplemental figure S1D–F). Considering that *Rag2*^{-/-} mice have

normal functioning dendritic cells (DCs), macrophages, natural killer (NK) cells and lack of CD8⁺ T cells, we hypothesised that the difference in tumour growth inhibition was not caused by DCs, macrophages and NK cells, but by T cells. Immunohistochemistry (IHC) showed enhanced infiltration of CD8⁺ T cells in CT26 tumour tissues from the MRD group (figure 1C, online supplemental figure S2B). Next, we evaluated the function of tumour-infiltrating CD8⁺ T cells by assessing their production of granzyme B (GZMB) and interferon- γ (IFN- γ) via flow cytometric analysis (online supplemental figure S2A). Compared with the CD group, the MRD group showed enhanced CD8⁺ T cells infiltration and stronger signals for both GZMB and IFN- γ in tumours and little difference in CD8⁺ T cells infiltration in spleen, draining lymph nodes and blood (figure 1D, online supplemental figure S2C–F). There was no difference in cytokine production or tumour infiltration of CD8⁺ T cells, but there was increased cytotoxicity between the MRD and CD groups (online supplemental figure S3A–C).

Gene set enrichment analysis revealed that pathways related to the immune response, such as the IFN- γ response and IFN- α response, were affected by the methionine restriction diet (figure 1E). Additionally, the effector CD8⁺ T cell signature was significantly enriched in the absence of methionine (figure 1F), indicating the involvement of an adaptive immune response in the MRD-mediated disruption of tumorigenesis. Thus, these results indicate that methionine deficiency inhibits tumour growth to some extent by enhancing tumour-infiltrating T cells in immunocompetent syngeneic mice.

To further determine whether MRD affects host antitumour immunity by strengthening T cell responses, we used the well-defined azoxymethane and dextran sodium sulfate (AOM-DSS) murine model to develop colitis-associated colon cancer (figure 1G). Moderately differentiated colon adenocarcinomas were observed in both groups (figure 1H). Notably, both the tumour number and size were dramatically decreased in MRD mice compared with those in CD mice (figure 1I). Additionally, MRD feeding significantly increased the level of CD8⁺ T lymphocytes in colon tumours (figure 1J, online supplemental figure S4A). To further explore the applicability of our findings, we used the xenograft-versus-host model of disease in which human peripheral blood mononuclear cells were infused into the circulation system of NOG mice, where human CD45⁺ cells, CD8⁺ T cells and functional CD8⁺ IFN- γ ⁺ T cells could be successfully detected, and the infiltration of these cells in spleen was not affected by the MRD feeding (online supplemental figure S4B,C). We then subcutaneously xenografted HCT116 and HT29 colon cancer cells into our humanised mouse model and observed that the tumour growth rate and tumour weight were significantly controlled in the context of MRD feeding (online supplemental figure S4D,E). As expected, the infiltration of CD8⁺ T cells was significantly increased in tumours in the MRD group (online supplemental figure S4F). Therefore, these data further confirm the repressive role of MRD in tumour development mediated via antitumour immunity.

Methionine is involved in a myriad of cellular functions. The metabolite analysis revealed that the MRD groups showed significant cysteine and methionine metabolic pathway-related metabolites in tumour tissues (figure 1K, online supplemental figure S5A). MRD feeding significantly reduced the levels of L-cystathionine (LCYH), SAM, S-adenosylhomocysteine (SAH), glutathione (GSH) and L-methionine (Met) in tumour tissues (figure 1L). Intracellular methionine is converted to SAM and then to SAH after transfer of the methyl group, which might be involved in the methylation levels of histone, DNA 5-mC and

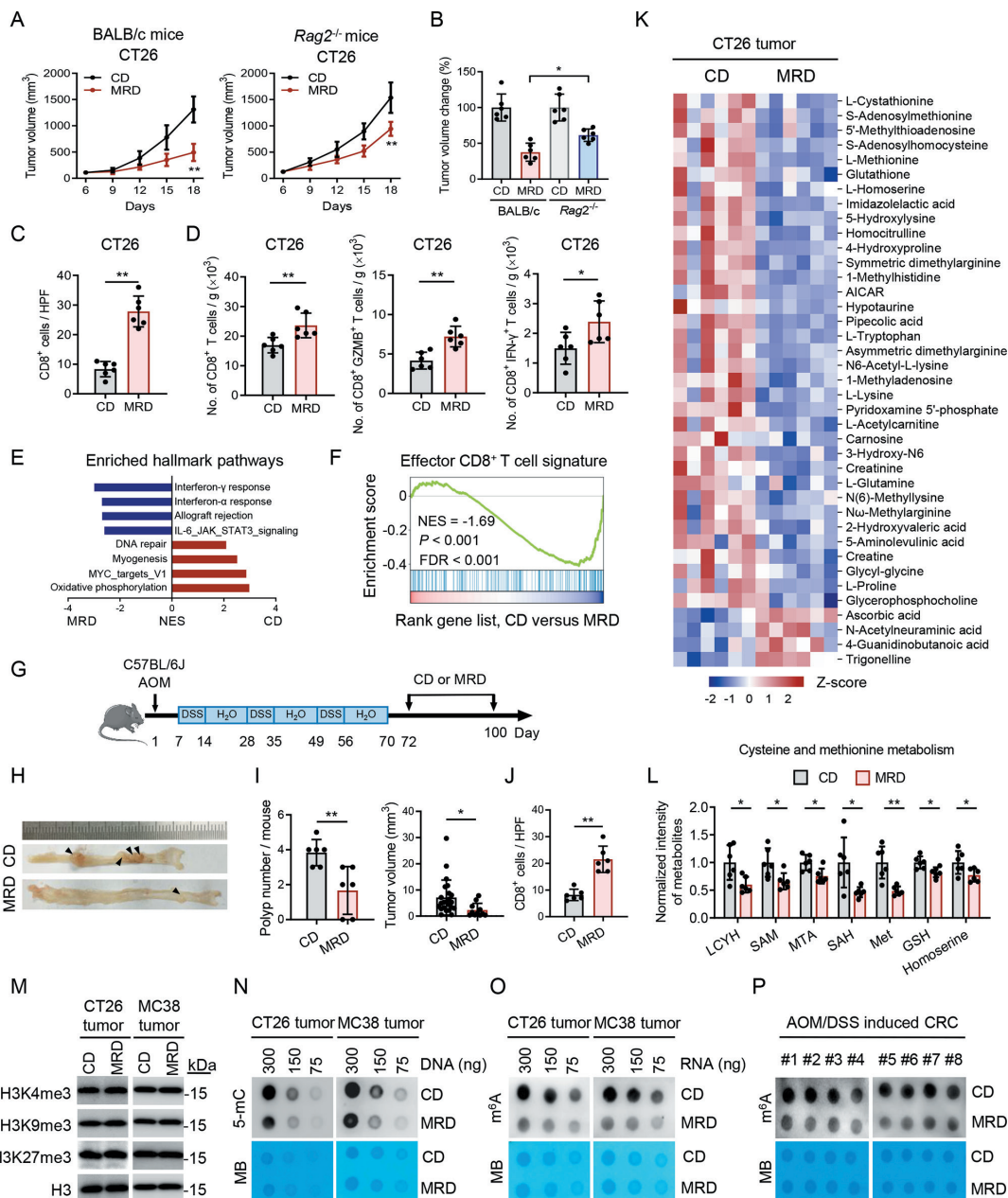


Figure 1 Methionine is critical for antitumour immunity. (A, B) Subcutaneous tumour models established in BALB/c mice and *Rag2*^{-/-} mice showing the tumour growth rate (A) and growth rate change (B) after implantation of CT26 cells with control diet (CD) or methionine-restricted diet (MRD) feeding (n=6 mice per group). (C) Quantification of CD8 staining in subcutaneous tumour model mice implanted with CT26 cells and subjected to CD or MRD feeding (n=6 mice per group). (D) Flow cytometric analysis of the number of CD8⁺ T cells, CD8⁺ GZMB⁺ T cells and CD8⁺ IFN- γ ⁺ T cells in subcutaneous tumour model mice implanted with CT26 cells and subjected to CD or MRD feeding (n=6 mice per group). (E) Pathway alterations in subcutaneous tumour model mice implanted with CT26 cells and subjected to CD or MRD feeding. (F) Gene set enrichment analysis of the effector CD8⁺ T cell signature in subcutaneous tumour implanted with CT26 cells and subjected to CD or MRD feeding. (G) Experimental design for the AOM-DSS induced mouse colon cancer model with CD or MRD feeding. (H, I) Representative images (H), tumour number (left) and tumour size (right) (I) of spontaneous colon tumours with CD or MRD feeding (n=6 mice per group). (J) Quantification of CD8 staining in the spontaneous mouse colon cancer model with CD or MRD feeding (n=6 mice per group). (K) Heatmap of changed metabolites in subcutaneous tumour model mice implanted with CT26 cells and subjected to CD or MRD feeding (n=6 mice per group). (L) Normalised intensities of LCYH, SAM, MTA, SAH, Met, GSH and homoserine in subcutaneous tumour model mice implanted with CT26 cells and subjected to CD or MRD feeding (n=6 mice per group). (M) Immunoblotting of H3K4me3, H3K9me3 and H3K27me3 from subcutaneous CT26 and MC38 tumours subjected to CD or MRD feeding. H3 was included as a loading control. (N) DNA dot blot assays of 5-mC in subcutaneous CT26 and MC38 tumours subjected to CD or MRD feeding. Methylene blue staining served as a loading control. (O) RNA m⁶A dot blot assays in subcutaneous CT26 and MC38 tumours subjected to CD or MRD feeding. Methylene blue staining served as a loading control. (P) RNA m⁶A dot blot assays in spontaneous mouse colon cancer model with CD or MRD feeding (300 ng). Methylene blue staining served as a loading control. The data in A–D, I, J and L are presented as the means \pm SDs. P values were determined by two-way ANOVA (A), one-way ANOVA (B) and two-tailed unpaired Student's t-test (C, D, I–L). *P<0.05; **P<0.01. ANOVA, analysis of variance; AOM, azoxymethane; CD, control diet; DSS, dextran sulfate sodium; GSH, glutathione; LCYH, L-cystathionine; MRD, methionine-restricted diet; 5-mC, 5-methylcytosine; MTA, 5'-methylthioadenosine; SAM, S-adenosylmethionine; SAH, S-adenosyl-L-homocysteine.

RNA m⁶A in bulk tumours (online supplemental figure S5B). As expected, MRD feeding influenced the above methylation reactions, among which 5-mC and m⁶A methylation were obviously reduced in bulk tumour cells (figure 1M–O, online supplemental figure S5C). Additionally, MRD feeding also decreased the RNA m⁶A methylation level in AOM-DSS induced colon tumours (figure 1P). Taken together, these results suggest that MRD feeding reduces the level of the methyl donor SAM in tumour tissues and may indirectly disrupt the effector functions of tumour-infiltrating T cells.

Methionine restriction enhances antitumour immunity via YTHDF1

Recent studies have shown that DNA 5-mC modification and RNA m⁶A modifications are regulated by a series of modulators that function as methyltransferases, demethylases and binding proteins, respectively.^{12–13} Through correlation analysis from The Cancer Genome Atlas (TCGA) database,^{14–15} we found that CD8⁺ T cell infiltration was negatively correlated with the expression of some regulators, among which the m⁶A-specific binding protein YTHDF1 exhibited the most significant negative correlation (online supplemental figure S6A). RNA m⁶A dot blot assays also showed that MRD feeding decreased the RNA m⁶A methylation level in GFP⁺ tumour cells sorted by flow cytometry (figure 2A). The downregulated IFN- γ response and effector CD8⁺ T cell signature in colorectal cancer (CRC) tumours with high YTHDF1 expression further supported the negative relationship between CD8⁺ T cell-mediated antitumour immunity and YTHDF1 expression (figure 2B,C). Additionally, the expression of YTHDF1 was negatively associated with TCR diversity, as denoted by TCR shannon entropy (figure 2D). IHC analysis verified that YTHDF1 expression was negatively associated with the infiltration of CD8⁺ T cells at the protein level (figure 2E). By analysing RNA-seq data on other types of cancers from TCGA, we further validated that similar negative relationships existed in various tumours (figure 2F), suggesting that YTHDF1 might act as an immune-inhibitory molecule for T cell functions in diverse tumours.

To test whether MRD affects T cell-mediated antitumour function via YTHDF1, we knocked down YTHDF1 (shYTHDF1#1, #2) in CT26 and MC38 cells, as confirmed by immunoblotting (online supplemental figure S6B). We initially compared cell growth in vitro and observed little difference in proliferation between YTHDF1-knockdown and vector control cells (online supplemental figure S6C). We then subcutaneously inoculated these cells into mice, fed the mice CD or MRD and observed the growth rate of tumours. Attenuation of YTHDF1 expression significantly inhibited tumour growth by CT26 cells and MC38 cells in BALB/c and C57BL/6J mice, respectively, in the context of CD feeding (figure 2G, online supplemental figure S6D,E). However, the inhibitory effect of YTHDF1 knockdown was counteracted in the context of MRD feeding (figure 2G, online supplemental figure S6D,E), implying the involvement of YTHDF1 in the MRD-mediated disruption of tumourigenesis. Additionally, we observed little difference in tumour growth between YTHDF1-knockdown and control tumours in immunodeficient *Rag2*^{-/-} mice (figure 2H, online supplemental figure S6F,G), suggesting the involvement of YTHDF1 in the adaptive immune response. Flow cytometric analysis revealed enhanced CD8⁺ T cell infiltration and increased functional CD8⁺ T cells in YTHDF1-knockdown tumour tissues inoculated in mice fed the CD compared with those fed the MRD (figure 2I,J, online supplemental figure S6H–J). Taken together, these data not only

demonstrate that YTHDF1 functions as an immunosuppressive molecule but also highlight a potential role for YTHDF1 in MRD-mediated antitumour efficiency by restricting T cell activation and increasing the cytotoxic potential.

To determine the repressive role of YTHDF1 in T cell responses and antitumour immunity, we generated conditional intestinal *Ythdf1* knockout mice (online supplemental figure S7A,B) from those mice containing floxed alleles of *Ythdf1* under the control of the *pVillin-Cre-ERT2* driver.^{16–17} To determine whether YTHDF1 is continuously required for tumour progression after tumour initiation, we administered tamoxifen after the final DSS treatment (figure 2K). After five tamoxifen treatments, *Ythdf1* was inducibly depleted in intestinal epithelial cells (online supplemental figure S7C). Remarkably, conditional depletion of *Ythdf1* during late stages in the AOM-DSS mouse model significantly reduced the multiplicity of large adenomas and load of total adenomas, exhibiting 50% reductions in both the tumour number and tumour volume compared with those of WT mice (figure 2L,M). H&E and IHC staining also showed that *Ythdf1*^{-/-} mice had less severe colon inflammation and higher amounts of CD8⁺ T cells than WT mice (figure 2N). Collectively, our data reveal that intestinal *Ythdf1*-deficient mice have reduced colon tumour formation when challenged with AOM-DSS.

Methionine and YTHDF1 promote the translation of PD-L1 and VISTA

The crosstalk between a tumour and the immune system drives a dynamic immunoeediting process that promotes cancer immune evasion.¹⁸ Hereafter, we performed RNA immunoprecipitation (RIP)-seq to analyse the recognised targets of YTHDF1. The results revealed that most YTHDF1 binding sites were located in protein-coding sequences (CDSs) and were highly enriched near stop codons and in 3' untranslated regions (figure 3A). By crossing the target genes with T cell-suppressive molecules in gastrointestinal cancer,¹⁹ we collected six molecules that might mediate the immunosuppressive function of YTHDF1 (figure 3B). Combining these findings with RIP-qPCR analysis, we identified the immunosuppressive molecules PD-L1 and VISTA as significant target genes of YTHDF1 (figure 3C). Immunoblot analysis and flow cytometric analysis indicated that the expression of PD-L1 and VISTA changed with YTHDF1 downregulation or overexpression (figure 3D,E, online supplemental figure S8A–C). These results suggest that YTHDF1 may regulate PD-L1 and VISTA expression in an m⁶A-dependent manner.

Methyltransferase-like protein (METTL) 3 and METTL14 are two critical components of the methyltransferase complex, which catalyses methylation at N⁶-adenosine.¹³ Consistent with the data on YTHDF1, knockdown of both METTL3 and METTL14 downregulated the expression of PD-L1 and VISTA in HCT116 and CT26 cells, as analysed by immunoblotting (figure 3F, online supplemental figure S8D,E). Additionally, the expression of PD-L1 and VISTA on the cell membrane was significantly decreased following METTL3/METTL14 complex depletion (figure 3G). Further investigation showed that methionine-restricted medium also reduced the expression levels of PD-L1 and VISTA (figure 3H, online supplemental figure S8F,G). Because IFN- γ is a major stimulator of PD-L1 expression through the IFN- γ -STAT1-PD-L1 signalling pathway in the tumour microenvironment,²⁰ we performed an IFN- γ stimulation assay and found increased PD-L1 protein levels in CRC cells following IFN- γ stimulation; these levels could be reduced by YTHDF1 knockdown or methionine restriction (figure 3I, online supplemental figure S8H). However, the

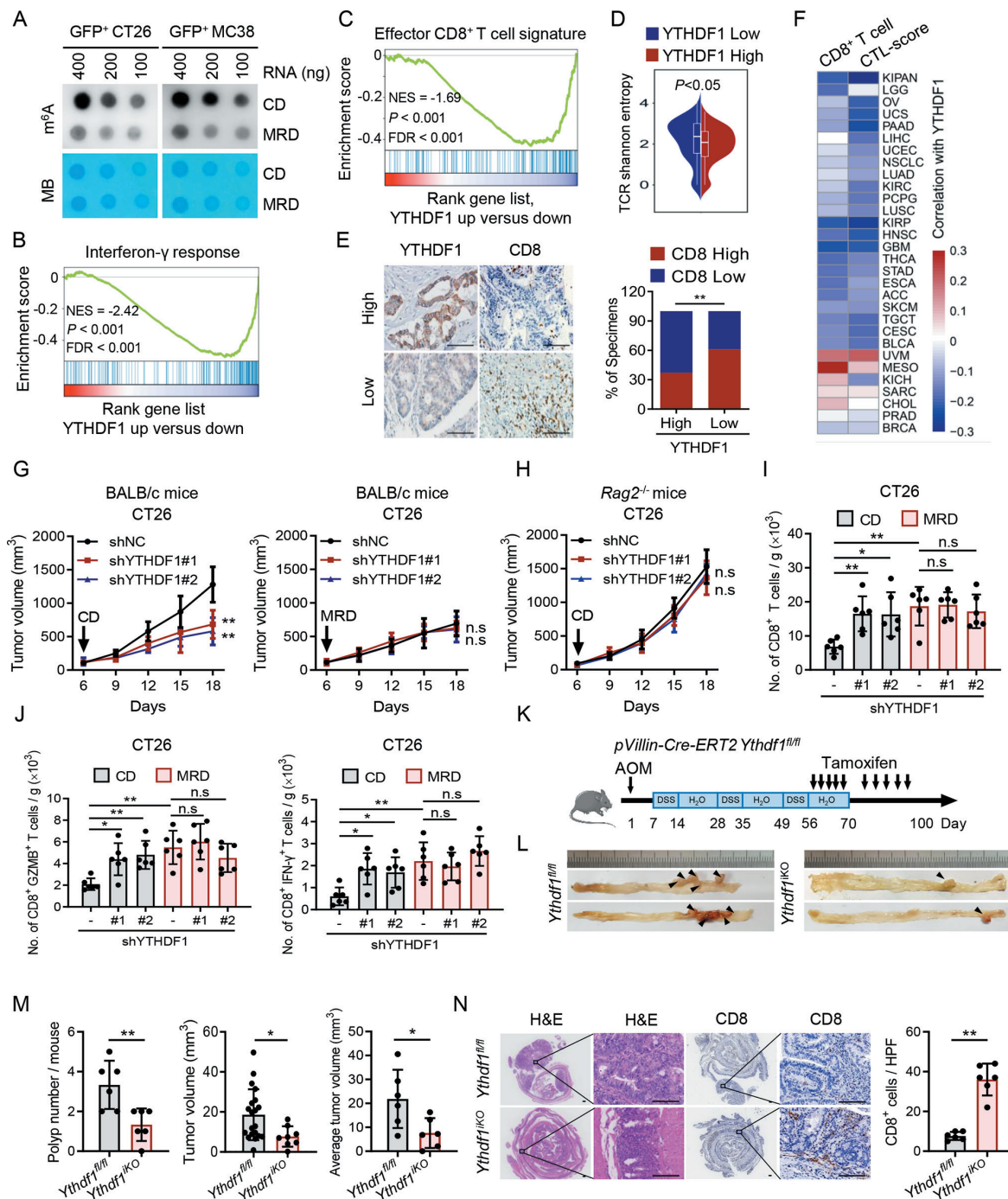


Figure 2 Methionine restriction enhances antitumour immunity via YTHDF1. (A) RNA m⁶A dot blot assays of GFP⁺ CT26 cells (left) and GFP⁺ MC38 cells (right) from subcutaneous tumours subjected to CD or MRD feeding. Methylene blue staining served as a loading control. (B, C) Gene set enrichment analysis of the interferon- γ response (B) and effector CD8⁺ T cell signature (C) in CRC with high or low expression of YTHDF1 in TCGA. (D) TCR Shannon entropy in data from TCGA for CRC with high or low expression of YTHDF1. (E) Representative images (left) and quantification (right) showing the correlation between YTHDF1 and CD8 in CRC microarray specimens (n=200, scale bar: 100 μ m). (F) Correlations of the CD8⁺ T cell infiltration or CTL score with YTHDF1 in other TCGA cancer types. (G) Subcutaneous tumour models showing the tumour growth rate after implantation of YTHDF1-knockdown or control CT26 cells with CD (left) or MRD (right) feeding in BALB/c mice (n=6 mice per group). (H) Subcutaneous tumour models showing the tumour growth rate after implantation of YTHDF1-knockdown or control cells in *Rag2*^{-/-} mice (n=6 mice per group). (I, J) Flow cytometric analysis of the number of CD8⁺ T cells, CD8⁺ GZMB⁺ T cells and CD8⁺ IFN- γ ⁺ T cells in subcutaneous tumour model mice implanted with YTHDF1-knockdown or control CT26 cells and subjected to CD or MRD feeding (n=6 mice per group). (K) Experimental design for the AOM-DSS induced mouse colon cancer model established in *Ythdf1*^{fl/fl} and *Ythdf1*^{iKO} mice. (L, M) Representative images (L), tumour number and tumour size (M) of spontaneous tumours in *Ythdf1*^{fl/fl} and *Ythdf1*^{iKO} mice. (N) Representative images (left) and quantification of H&E and CD8 staining (right) in a spontaneous mouse colon cancer model established in *Ythdf1*^{fl/fl} and *Ythdf1*^{iKO} mice (scale bar: 100 μ m) (n=6 mice per group). The data in G–J, M and N are presented as the means \pm SDs. P values were determined by Pearson's χ^2 test (E), two-way ANOVA (G–H), one-way ANOVA (I–J) and two-tailed unpaired Student's t-test (M, N). *P<0.05; **P<0.01; ANOVA, analysis of variance; AOM, azoxymethane; CD, control diet; CRC, colorectal cancer; CTL, cytotoxic T lymphocyte; DSS, dextran sodium sulfate; n.s., not significant; TCGA, The Cancer Genome Atlas.

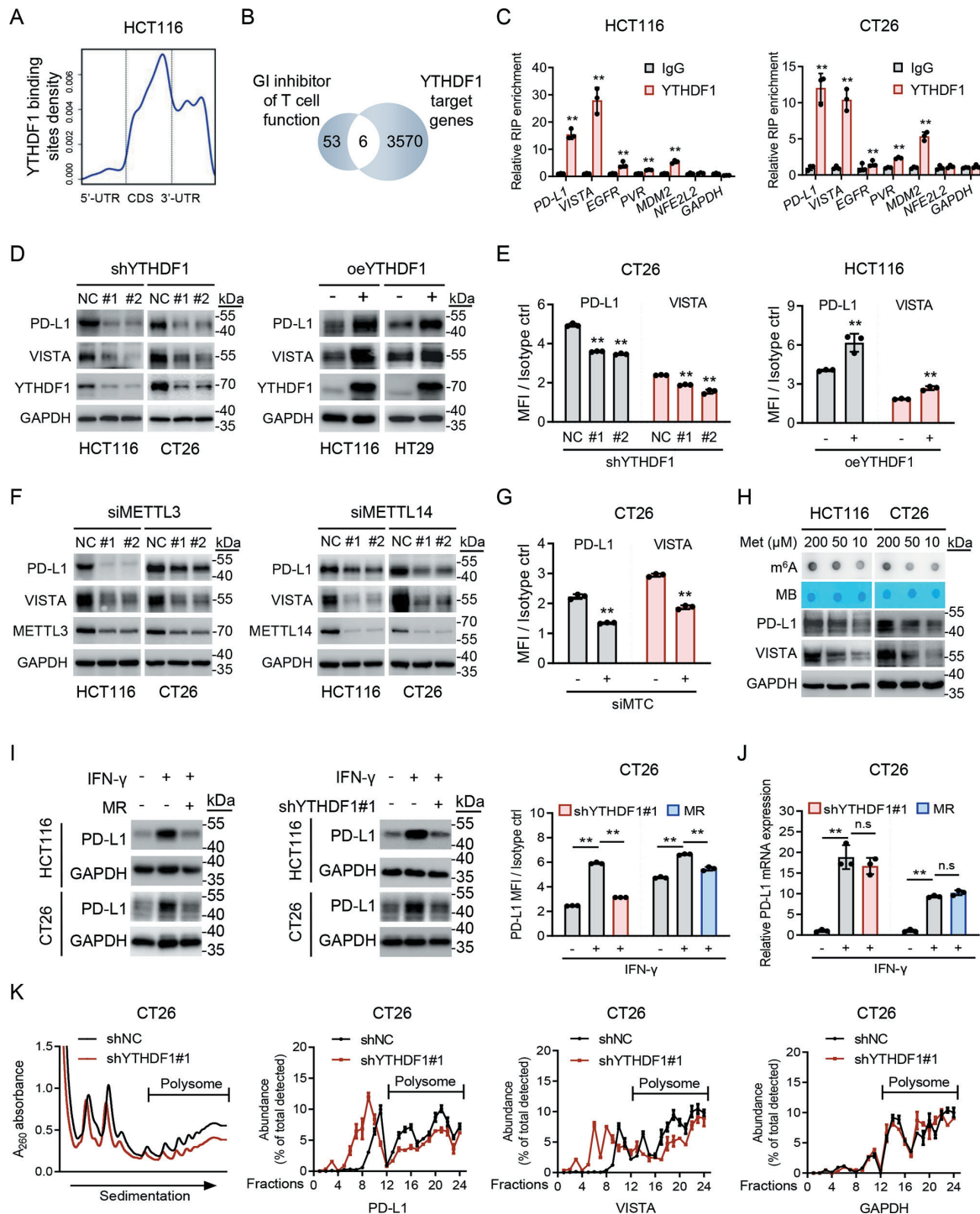


Figure 3 Methionine and YTHDF1 promote the translation of PD-L1 and VISTA. (A) Metagene plot of the density of YTHDF1 binding sites in HCT116 cells. (B) Venn diagram showing the shared genes between T cell function suppressors in gastrointestinal (GI) cancer and YTHDF1 target genes. (C) RIP assays in CRC cells showing the direct binding between the YTHDF1 protein and PD-L1, VISTA, EGFR, PVR, MDM2 and NFE2L2 transcripts. (D) Immunoblotting of PD-L1 and VISTA after YTHDF1 inhibition (left) or overexpression (right) in CRC cells. GAPDH was included as a loading control. (E) Flow cytometric analysis of PD-L1 and VISTA after YTHDF1 inhibition (left) or overexpression (right) in CRC cells. (F) Immunoblotting of PD-L1 and VISTA after METTL3 (left) or METTL14 (right) inhibition in CRC cells. GAPDH was included as a loading control. (G) Flow cytometric analysis of PD-L1 and VISTA after MTC inhibition in CT26 cells. (H) RNA m⁶A dot blot assays and immunoblotting of PD-L1 and VISTA in CRC cells subjected to methionine restriction. Methylene blue staining and GAPDH served as a loading control. (I) Immunoblotting (left) and flow cytometric analyses (right) of PD-L1 after methionine restriction (MR) or YTHDF1 inhibition with IFN- γ stimulation in CRC cells. GAPDH was included as a loading control. (J) qPCR analysis of PD-L1 expression after MR or YTHDF1 inhibition with IFN- γ stimulation in CT26 cells. (K) Polysome profiles and qPCR analysis of YTHDF1-knockdown or control CT26 cells on a 5%–50% sucrose gradient. The data in C, E, G, I, J and K are presented as the means \pm SDs. P values were determined by two-tailed unpaired Student's t-test (C, HCT116 in E and G) and one-way ANOVA (CT26 in E, I, and J). **P<0.01; n.s, not significant. ANOVA, analysis of variance; CRC, colorectal cancer; MFI, mean fluorescence intensity; MTC, methyltransferase complex; RIP, RNA immunoprecipitation.

mRNA level could not be rescued (figure 3J). YTHDF1, an m⁶A reader protein, directly promotes the translation of methylated mRNAs.²¹ Thus, we evaluated the mRNA levels and found that neither YTHDF1 knockdown nor methionine restriction affected the transcriptional levels of PD-L1 and VISTA (online supplemental figure S8I,J). Finally, polysome profiling demonstrated that YTHDF1 knockdown resulted in a decreased polysome fraction and a moderate shift in PD-L1 and VISTA mRNAs to nonpolysome fractions, resulting in reduced translation efficiency of PD-L1 and VISTA mRNA (figure 3K). These results indicate that YTHDF1 promotes the protein synthesis of PD-L1 and VISTA.

YTHDF1 regulates PD-L1 and VISTA expression in an m⁶A-dependent manner

Then, RIP-qPCR using a YTHDF1-specific antibody demonstrated strong binding between YTHDF1 and PD-L1 or VISTA mRNA that could be significantly suppressed by methionine restriction or METTL3/METTL14 complex knockdown in HCT116 cells and CT26 cells (figure 4A,B). By analysing the RIP-seq data and predicting the m⁶A motifs of PD-L1 and VISTA transcripts using the SRAMP tool (<http://www.cuilab.cn/sramp>), we selected three potential binding regions with potential m⁶A sites in both PD-L1 (P1, P2, P3) and VISTA (V1, V2, V3) transcripts (figure 4C) and conducted MeRIP-qPCR and CLIP-qPCR for further verification. m⁶A modification of PD-L1 mainly occurred and was recognised by YTHDF1 at sites P1 and P3, while that of VISTA mainly occurred at sites V2 and V3 (figure 4D,E, online supplemental figure S9A). Additionally, reducing the methionine concentration in the medium significantly abrogated the interactions between YTHDF1 and these binding sites (figure 4F,G). Finally, we performed in vitro and in vivo RNA pull-down experiments to verify the binding in the reverse manner. The in vitro assay revealed that PD-L1 and VISTA RNA oligos with m⁶A modifications added to the consensus sites during synthesis could bind YTHDF1 (figure 4H, online supplemental figure S9B). Additionally, a point mutation in the m⁶A sites (A to T) of the PD-L1 and VISTA RNA probes dramatically abrogated the binding between YTHDF1 proteins and these RNA probes in vivo (figure 4I). Taken together, our data identify the specific m⁶A binding sites in PD-L1 and VISTA mRNA transcripts recognised by YTHDF1.

MRD or YTHDF1 depletion synergises with PD-1 blockade

Based on the above findings, we further investigated whether restricting methionine from the diet or depleting YTHDF1 enhances the antitumour activity of ICB therapy in mouse models. We first tested whether methionine restriction synergises with PD-1 blockade. BALB/c mice bearing CT26 tumours were subjected to CD or MRD feeding when tumours were palpable and then treated with control IgG or anti-PD-1 antibody. The anti-PD-1 antibody had a limited effect on CT26 tumour growth compared with the control IgG antibody (figure 5A), consistent with a previous study finding.²² Interestingly, dietary methionine restriction synergised with anti-PD-1 treatment, leading to marked inhibition of tumour growth and a significant decrease in tumour weight (figure 5A, online supplemental figure S10A). These effects were accompanied by increased CD8⁺ T cell infiltration in tumours (figure 5A). Next, YTHDF1-knockdown and control CT26 cells were subcutaneously injected into BALB/c mice with control IgG or anti-PD-1 antibody treatment. Compared with those bearing control tumours, mice-bearing YTHDF1-knockdown CT26 tumours showed slower tumour

growth, decreased tumour weight and increased CD8⁺ T cell infiltration (figure 5B, online supplemental figure S10B). Similar results were also observed using the MC38 subcutaneous tumour model with either dietary methionine restriction or YTHDF1 knockdown (figure 5C,D, online supplemental figure S10C,D). Furthermore, the OS of mice receiving the combination therapy was significantly prolonged compared with that of mice in either monotherapy group (figure 5E,F).

YTHDF1 correlates with poor prognosis and immunotherapy outcomes

Finally, we examined the potential relationship between YTHDF1 expression and clinical outcome in CRC patients. Based on available TCGA data, we found that YTHDF1 transcripts were higher in several tumour tissues than in matched normal tissues (online supplemental figure S10E). We next examined YTHDF1 expression in a cohort of CRC tissues from our hospital (Sun Yat-Sen University Cancer Center) by RT-qPCR and IHC. The results showed that YTHDF1 was not only upregulated in CRC tissues but also elevated in recurrent CRC tissues (figure 5G,H). MeRIP-qPCR also confirmed that the m⁶A modification levels of PD-L1 and VISTA transcripts were significantly increased in CRC tissues (figure 5I). Strikingly, Kaplan–Meier survival analysis indicated that patients with high YTHDF1 expression levels had shorter OS and disease-free survival (DFS) (figure 5J). Multivariate analysis also indicated that YTHDF1 expression was an independent prognostic factor in CRC patients, suggesting that YTHDF1 is a potential prognostic biomarker (online supplemental table S1). Considering the association between YTHDF1 and antitumour immunity, we also examined the correlation between YTHDF1 expression and clinical outcome in patients receiving immunotherapy from three published immunotherapy RNA-seq cohorts.^{23–25} As expected, a significantly shorter OS was observed in patients exhibiting high YTHDF1 expression levels in pretreatment samples (figure 5K). Additionally, patients who exhibited high YTHDF1 expression levels in on-treatment samples still exhibited worse OS (figure 5K). Thus, the YTHDF1 expression level has the potential to distinguish patients who could derive greater benefit from ICB.

DISCUSSION

Emerging evidence indicates that cancer metabolism not only plays crucial roles in tumorigenesis and progression but also has wider implications for regulating the antitumour immune response. Cancer cells can suppress the antitumour immune response by competing with tumour-infiltrating immune cells for essential nutrients.^{26–27} On the other hand, aberrant intermediates of cancer metabolism also have profound effects on immune cells in the microenvironment.^{28–31} A previous study by Bian *et al* showed that tumour cells disrupt methionine metabolism in CD8⁺ T cells, thereby decreasing intracellular levels of methionine, and resulting in the impaired T cell immunity. Additionally, methionine supplementation increased T cell immunity in tumour-bearing mice and patients with colon cancer.¹¹ We now show that dietary methionine restriction results in decreases in a series of metabolites in cancer cells, including SAM, which controls the flux of the m⁶A methylation reactions. These changes enhance antitumour efficiency and improve the clinical outcome of ICB therapies by controlling the expression of immune checkpoint inhibitors (ICIs), PD-L1 and VISTA, in an m⁶A-dependent manner. Our work are also consistent with other reports that MRD inhibits tumour growth.^{8–32–34} The methionine restriction diet adopted in our study is different from the

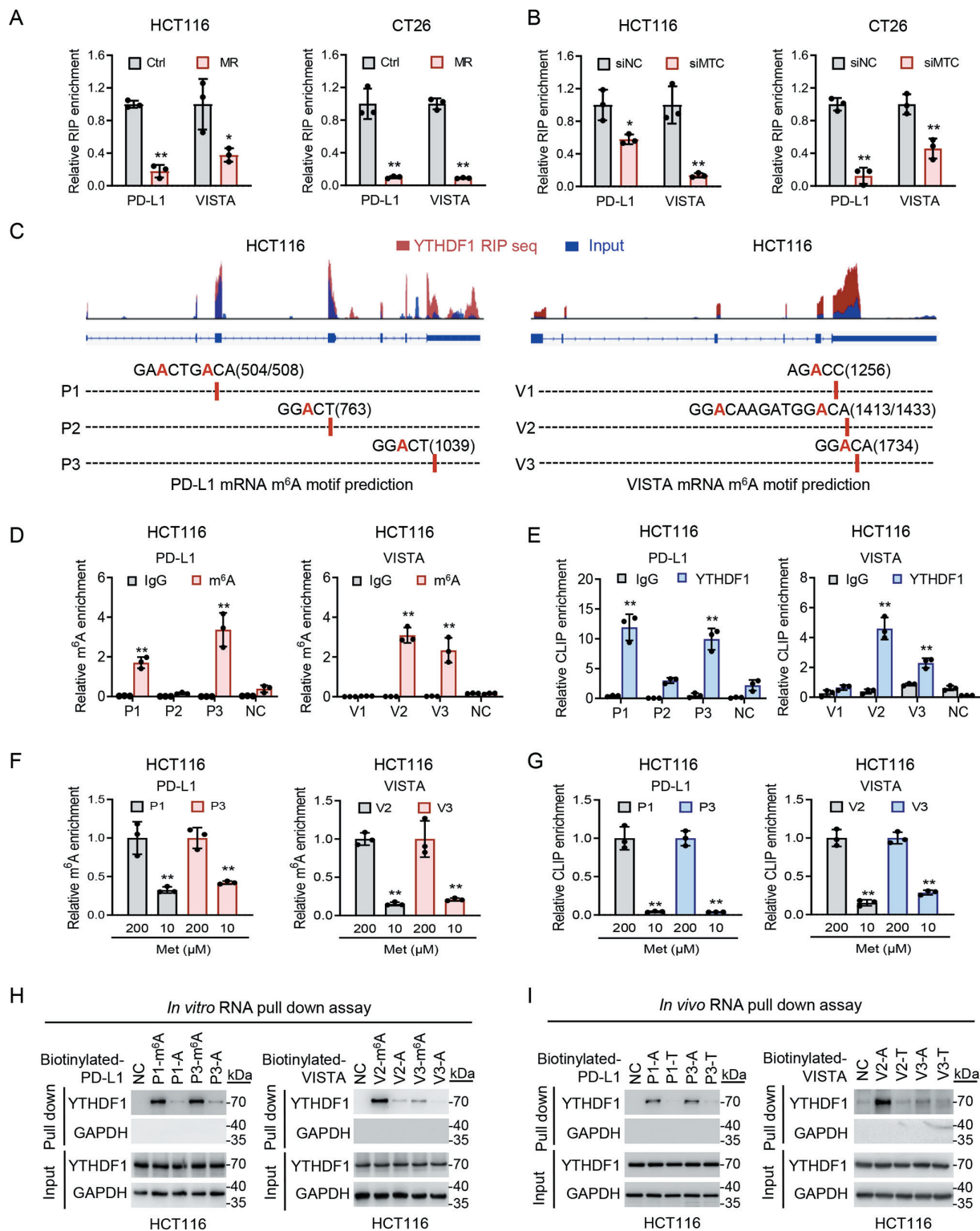


Figure 4 YTHDF1 regulates PD-L1 and VISTA expression in an m⁶A-dependent manner. (A, B) RIP enrichment of PD-L1 and VISTA mRNAs after MR (A) or MTC inhibition (B) in CRC cells. (C) Distribution of YTHDF1 binding peaks and m⁶A motif prediction across PD-L1 and VISTA transcripts in HCT116 cells. (D) MeRIP-qPCR analysis of specific m⁶A motif enrichment in PD-L1 (left) and VISTA (right) mRNAs in HCT116 cells. (E) CLIP-qPCR analysis of specific YTHDF1 binding enrichment in PD-L1 (left) and VISTA (right) mRNAs in HCT116 cells. (F) MeRIP-qPCR analysis of specific m⁶A motif enrichment in PD-L1 (left) and VISTA (right) mRNAs after methionine restriction in HCT116 cells. (G) CLIP-qPCR analysis of specific YTHDF1 binding enrichment in PD-L1 (left) and VISTA (right) mRNAs after methionine restriction in HCT116 cells. (H, I) *In vitro* and *in vivo* RNA pull-down assays for YTHDF1 binding to biotinylated PD-L1 (left) probes or biotinylated VISTA (right) probes in HCT116 cells. GAPDH was included as a loading control. The data in A, B, D–G are presented as means±SDs. P values were determined by two-tailed unpaired Student's t-test (A, B, D–G). *P<0.05, **P<0.01. CRC, colorectal cancer; MTC, methyltransferase complex.

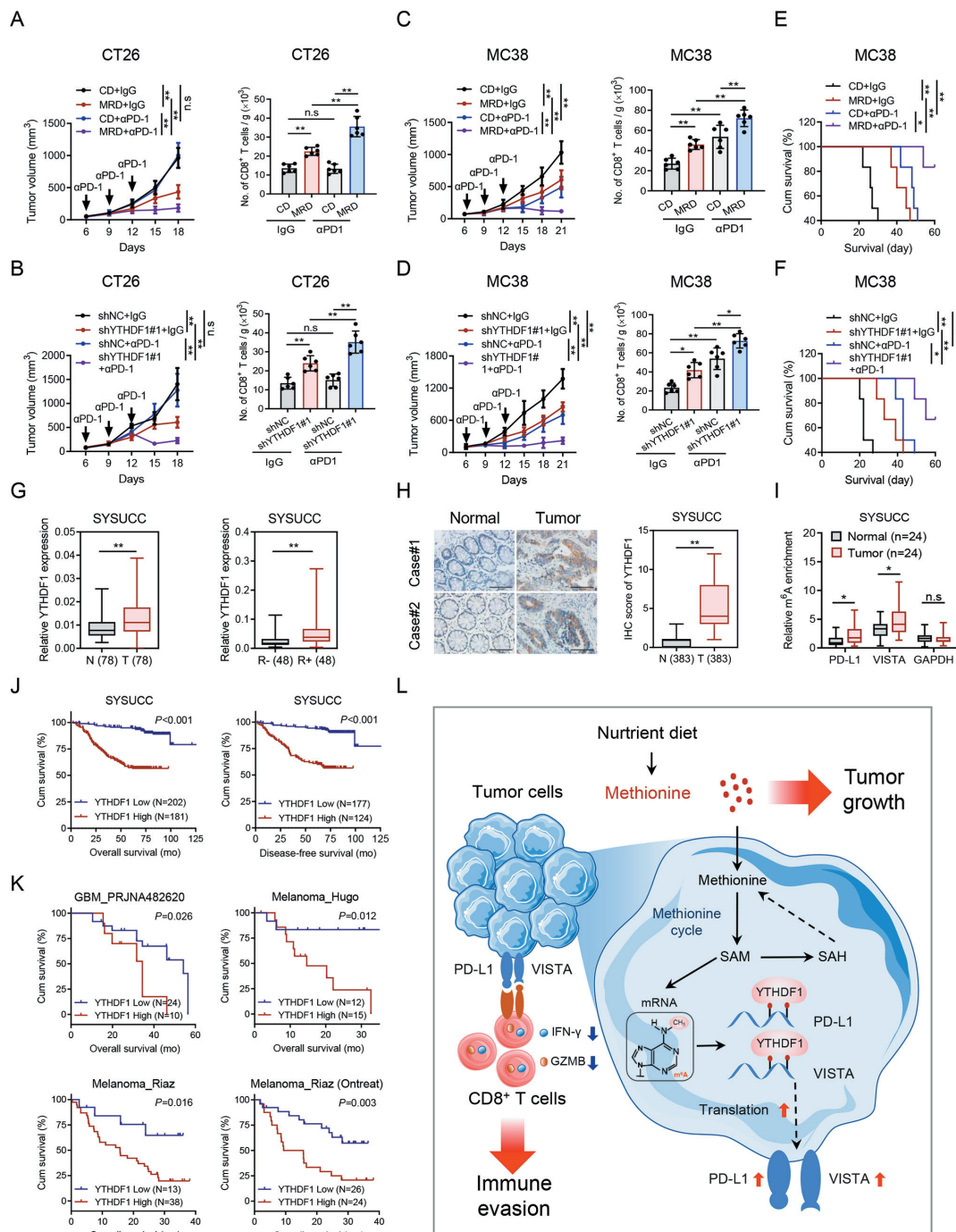


Figure 5 MRD feeding or YTHDF1 depletion synergises with PD-1 blockade and has clinical implications. (A) CT26 subcutaneous tumour growth and flow cytometric analysis of the number of CD8⁺ T cells with CD or MRD feeding treated with IgG or αPD-1 (n=6 mice per group). (B) Subcutaneous tumour growth and flow cytometric analysis of the number of CD8⁺ T cells with YTHDF1-knockdown or control CT26 cells treated with IgG or αPD-1 (n=6 mice per group). (C) MC38 subcutaneous tumour growth and flow cytometric analysis of the number of CD8⁺ T cells with CD or MRD feeding treated with IgG or αPD-1 (n=6 mice per group). (D) Subcutaneous tumour growth and flow cytometric analysis of the number of CD8⁺ T cells with YTHDF1-knockdown or control MC38 cells treated with IgG or αPD-1 (n=6 mice per group). (E, F) Kaplan-Meier analysis of the survival of C57BL/6J mice in the indicated groups (n=6 mice per group). (G) qPCR analysis of YTHDF1 expression in CRC tissues from paired adjacent normal tissues (N, n=78) and primary tumour samples (T, n=78), and from patients without recurrence (R-, n=48) and with recurrence (R+, n=48) at SYSUCC. (H) Representative IHC images and quantification of YTHDF1 in CRC-adjacent normal tissues vs CRC tumour tissues (scale bar: 100 μm, n=383). (I) MeRIP-qPCR assays of the m⁶A enrichment of PD-L1 and VISTA mRNAs in 24 paired CRC primary tumour samples and adjacent normal tissue samples. (J) Kaplan-Meier analysis of overall survival (OS) and disease-free survival (DFS) based on YTHDF1 expression in the SYSUCC cohort. (K) Kaplan-Meier analysis of OS or DFS based on YTHDF1 expression in published ICI treatment cohorts. (L) Working model of the proposed mechanism in this study. The data in A–D are presented as the means ± SDs. The data in E, F, J and K were determined by Kaplan-Meier analysis with the log-rank test. The data in G–I are presented as a box-and-whisker graph (min-max), and the horizontal line across the box indicates the median. P value was determined by two-way ANOVA (tumour volume in A–D), one-way ANOVA (NO. of CD8⁺ T cells / g (× 10³) in A–D) and two-tailed unpaired Student's t-test (G–I). *P < 0.05; **P < 0.01; n.s., not significant. ANOVA, analysis of variance; ICI, immune checkpoint inhibitor.

complete methionine deficiency or methionine supplementation by intratumour injection used in Bian *et al*'s study, which might be the reason for the different results between our studies. Our findings highlight a novel role for methionine in regulating the antitumour immune response, among which m⁶A is the major factor, further suggesting that metabolic interventions hold promise for improving the effectiveness of immunotherapies. Beyond the fundamental role of methionine restriction and m⁶A in antitumour immunity, there may be other mechanisms to which tumour inhibition likely contributes, such the alterations of immune components in methionine restriction effects and histone K4/9/27me3 methylation, which are worth in-depth study.

Tumours have hijacked inhibitory checkpoints to evade immune-mediated eradication. Recent studies have identified several immune checkpoint molecules in cancer, including PD-1, PD-L1, cytotoxic T-lymphocyte associated protein 4 (CTLA-4), VISTA, and lymphocyte activating 3 (LAG3).^{35–36} Among these, PD-1/PD-L1, the most well-known ICIs, have realised the transformation from the laboratory to clinical application.^{33,37} VISTA, a newly emerging ICI, is a novel B7 family member that suppresses T cell activation for immune evasion and tumour progression in several human cancers with PD-1-independent immune evasion mechanisms, making it a promising target for combination cancer immunotherapy.^{38,39} Interestingly, some studies have suggested that the immunosuppressive role of VISTA may be the potential mechanism for acquired drug resistance in melanoma patients treated with anti-PD-1 antibodies.^{40,41} In our data, MRD or YTHDF1 depletion both reduced the expression of PD-L1 and VISTA, so VISTA still played an important immunosuppressive role even when the PD-1/PD-L1 pathway was blocked by anti-PD-1 treatment. This finding partly explains why combined treatment with PD-1 blockade in MRD or YTHDF1 depletion can reverse immunotherapy tolerance of CT26 cold tumours and augment the immunotherapy response of MC38 hot tumours.

Obviously, elucidating the function and regulatory mechanism of these ICIs is beneficial for developing effective strategies for tumour immunotherapy. According to the literature, the expression of PD-L1 and VISTA is regulated by multiple transcriptional and posttranslational mechanisms.^{35,42} Additionally, VISTA expression is transcriptionally upregulated by the transcription factors forkhead box D3 (FOXD3) and hypoxia-inducible factor 1 α (HIF-1 α).^{43,44} Our present study provides a novel regulatory mechanism by which YTHDF1 recognises m⁶A-containing mRNA transcripts of PD-L1 and VISTA and enhances their translation efficiency. Furthermore, we elucidated the regulatory mechanisms of PD-L1 and VISTA from the perspective of epigenetic RNA modification and posttranscriptional regulation, adding new scientific content to understanding the regulation of immune checkpoint molecules.

Despite the arousing achievements of ICB therapies in recent years, the overall response rates of ICB therapies remain unsatisfactory in some specific tumour types and cancer patients. It is urgent to verify effective markers to distinguish patients who could actually benefit from ICB therapies. The ever-increasing understanding of RNA m⁶A modification in the tumour immune microenvironment facilitates the development of immunotherapies and the identification of novel predictive markers for ICB therapies.⁴⁵ Recent studies have indicated that the m⁶A methyltransferase METTL3 is a positive regulator of macrophage activation^{46,47} and that METTL14 in tumour-associated macrophages (TAMs) promotes CD8⁺ T cell dysfunction and tumour progression.⁴⁸ In addition to these studies on macrophages, recent studies have also reported that the m⁶A methylation programme

orchestrates cancer growth and immune escape by regulating the functions of tumour cells, DCs, NK cells and others.⁴⁹ Furthermore, m⁶A-related molecules, such as METTL3, METTL14 and ALKBH5, are involved in regulating the response to anti-PD-1 therapy,^{22,50} serving as potential predictive biomarkers for immunotherapy. Our present study not only reveals a novel regulatory mechanism of RNA m⁶A modification involved in antitumour immunity, but also highlights that the combination strategy of methionine restriction with anti-PD-1 treatment based on the difference in YTHDF1 expression for patient selection can produce promising survival benefits.

As indicated by the data from our working models (figure 5L), our study enriches our understanding of the mechanistic connections among methionine metabolism, RNA m⁶A methylation and antitumour immunity in tumour progression. First, methionine plays critical roles in anticancer immunity and the functions of T cells by providing a methyl donor for RNA m⁶A modification. Second, the epigenetic regulatory mechanism of YTHDF1 involves regulating the expression of immune checkpoint molecules, showing that YTHDF1 is a novel potential biomarker for immunotherapy outcomes. Given that dietary methionine restriction synergises with PD-1 blockade in diverse mouse models, further investigation of dietary methionine interventions may shed light on new strategies for cancer immunotherapy.

Author affiliations

¹State Key Laboratory of Oncology in South China, Collaborative Innovation Center for Cancer Medicine, Sun Yat-sen University Cancer Center, Guangzhou, Guangdong, China

²Department of Gastroenterology and Urology, Hunan Cancer Hospital/The Affiliated Cancer Hospital of Xiangya School of Medicine, Central South University, Changsha, Hunan, China

³Research Department of Medical Sciences, Guangdong Provincial People's Hospital, Guangdong Academy of Medical Sciences, Guangzhou, Guangdong, China

⁴CAS Key Laboratory of Separation Science for Analytical Chemistry, Dalian Institute of Chemical Physics, Chinese Academy of Sciences, Dalian, Liaoning, China

⁵Department of Colorectal Surgery, Sun Yat-sen University Cancer Center, Guangzhou, Guangdong, China

⁶Guangdong Provincial Key Laboratory of Molecular Oncologic Pathology, Southern Medical University, Guangzhou, Guangdong, China

⁷Research Unit of Precision Diagnosis and Treatment for Gastrointestinal Cancer, Chinese Academy of Medical Sciences, Guangzhou, Guangdong, China

Acknowledgements We thank Human Metabolome Technologies Inc. (HMT, Japan) and Agilent Technologies Inc. (USA) for their technical support.

Contributors H-QJ and R-HX designed the study. TL, Y-TT, Y-XC, X-JZ, KL, WW, H-YM and JL collected the data. H-QJ, TL, Y-TT and Y-XC analysed and interpreted the data. TL, Y-TT and Y-XC performed the statistical analysis. H-QJ, TL and Y-TT wrote the manuscript. H-LP and WY contributed to discussion and data interpretation. H-QJ, R-HX, H-LP, TL, Y-TT and X-JZ revised the manuscript. H-QJ supervised and accepted full responsibility for the work as the guarantor. All authors reviewed the manuscript and approved the final version. The findings of this study are available from the corresponding authors on reasonable request.

Funding This research was supported by the National Natural Science Foundation of China (82022052, 81871951), Natural Science Foundation of Guangdong Province (2019A1515010233), Science and Technology Program of Guangzhou (201904020046), Beijing Science and Technology Innovation Medical Development Foundation (KC2021-JX-0186-65) and CAMS Innovation Fund for Medical Sciences (2019-I2M-5-036).

Competing interests None declared.

Patient and public involvement Patients and/or the public were not involved in the design, or conduct, or reporting, or dissemination plans of this research.

Patient consent for publication Not applicable.

Ethics approval All tissue chips were obtained with approval by the Institutional Research Ethics Committee of SYSUCC. All animal studies were performed in accordance with a protocol approved by the Institutional Ethics Committee for Clinical Research and Animal Trials of the SYSUCC. The ethics approval ID is GZR2020-189.

Provenance and peer review Not commissioned; externally peer reviewed.

Data availability statement Data are available in a public, open access repository. Data are available on reasonable request. All data relevant to the study are included in the article or uploaded as online supplemental information. RNA-seq data and RIP-seq data are available in Sequence Read Archive (SRA) PRJCA006189 (<http://bigd.big.ac.cn/gsa-human/>).

Supplemental material This content has been supplied by the author(s). It has not been vetted by BMJ Publishing Group Limited (BMJ) and may not have been peer-reviewed. Any opinions or recommendations discussed are solely those of the author(s) and are not endorsed by BMJ. BMJ disclaims all liability and responsibility arising from any reliance placed on the content. Where the content includes any translated material, BMJ does not warrant the accuracy and reliability of the translations (including but not limited to local regulations, clinical guidelines, terminology, drug names and drug dosages), and is not responsible for any error and/or omissions arising from translation and adaptation or otherwise.

Open access This is an open access article distributed in accordance with the Creative Commons Attribution Non Commercial (CC BY-NC 4.0) license, which permits others to distribute, remix, adapt, build upon this work non-commercially, and license their derivative works on different terms, provided the original work is properly cited, appropriate credit is given, any changes made indicated, and the use is non-commercial. See: <http://creativecommons.org/licenses/by-nc/4.0/>.

ORCID iDs

Rui-Hua Xu <http://orcid.org/0000-0001-9657-4380>

Huai-Qiang Ju <http://orcid.org/0000-0003-1713-5465>

REFERENCES

- Topalian SL, Taube JM, Pardoll DM. Neoadjuvant checkpoint blockade for cancer immunotherapy. *Science* 2020;367:eaax0182.
- Hegde PS, Chen DS. Top 10 challenges in cancer immunotherapy. *Immunity* 2020;52:17–35.
- Luo H, Lu J, Bai Y, et al. Effect of Camrelizumab vs placebo added to chemotherapy on survival and progression-free survival in patients with advanced or metastatic esophageal squamous cell carcinoma. *JAMA* 2021;326:916–25.
- Samstein RM, Lee C-H, Shoushtari AN, et al. Tumor mutational load predicts survival after immunotherapy across multiple cancer types. *Nat Genet* 2019;51:202–6.
- Wang F, Zhao Q, Wang Y-N, et al. Evaluation of *POLE* and *POLD1* Mutations as Biomarkers for Immunotherapy Outcomes Across Multiple Cancer Types. *JAMA Oncol* 2019;5:1504–6.
- Muthusamy T, Cordes T, Handzlik MK, et al. Serine restriction alters sphingolipid diversity to constrain tumour growth. *Nature* 2020;586:790–5.
- Meadows GG, Pierson HF, Abdallah RM, et al. Dietary influence of tyrosine and phenylalanine on the response of B16 melanoma to carbidopa-levodopa methyl ester chemotherapy. *Cancer Res* 1982;42:3056–63.
- Gao X, Sanderson SM, Dai Z, et al. Dietary methionine influences therapy in mouse cancer models and alters human metabolism. *Nature* 2019;572:397–401.
- Mentch SJ, Mehrmohamadi M, Huang L, et al. Histone methylation dynamics and gene regulation occur through the sensing of one-carbon metabolism. *Cell Metab* 2015;22:861–73.
- Sanderson SM, Gao X, Dai Z, et al. Methionine metabolism in health and cancer: a nexus of diet and precision medicine. *Nat Rev Cancer* 2019;19:625–37.
- Bian Y, Li W, Kremer DM, et al. Cancer SLC43A2 alters T cell methionine metabolism and histone methylation. *Nature* 2020;585:277–82.
- Michalak EM, Burr ML, Bannister AJ, et al. The roles of DNA, RNA and histone methylation in ageing and cancer. *Nat Rev Mol Cell Biol* 2019;20:573–89.
- Huang H, Weng H, Chen J. m6A modification in coding and non-coding RNAs: roles and therapeutic implications in cancer. *Cancer Cell* 2020;37:270–88.
- Cancer Genome Atlas Research Network, Weinstein JN, Collisson EA, et al. The cancer genome atlas pan-cancer analysis project. *Nat Genet* 2013;45:1113–20.
- Newman AM, Steen CB, Liu CL, et al. Determining cell type abundance and expression from bulk tissues with digital cytometry. *Nat Biotechnol* 2019;37:773–82.
- Madison BB, Dunbar L, Qiao XT, et al. Cis elements of the villin gene control expression in restricted domains of the vertical (crypt) and horizontal (duodenum, cecum) axes of the intestine. *J Biol Chem* 2002;277:33275–83.
- el Marjou F, Janssen K-P, Chang BH-J, et al. Tissue-Specific and inducible Cre-mediated recombination in the gut epithelium. *Genesis* 2004;39:186–93.
- Wellenstein MD, de Visser KE. Cancer-Cell-Intrinsic mechanisms shaping the tumor immune landscape. *Immunity* 2018;48:399–416.
- Ru B, Wong CN, Tong Y, et al. TISIDB: an integrated Repository portal for tumor-immune system interactions. *Bioinformatics* 2019;35:4200–2.
- Lv H, Lv G, Chen C, et al. NAD⁺ Metabolism Maintains Inducible PD-L1 Expression to Drive Tumor Immune Evasion. *Cell Metab* 2021;33:110–27.
- Wang X, Zhao BS, Roundtree IA, et al. N(6)-methyladenosine Modulates Messenger RNA Translation Efficiency. *Cell* 2015;161:1388–99.
- Wang L, Hui H, Agrawal K, et al. m⁶A RNA methyltransferases METTL3/14 regulate immune responses to anti-PD-1 therapy. *Embo J* 2020;39:e104514.
- Hugo W, Zaretsky JM, Sun L, et al. Genomic and transcriptomic features of response to anti-PD-1 therapy in metastatic melanoma. *Cell* 2016;165:35–44.
- Riaz N, Havel JJ, Makarov V, et al. Tumor and microenvironment evolution during immunotherapy with nivolumab. *Cell* 2017;171:934–49.
- Zhao J, Chen AX, Gartrell RD, et al. Immune and genomic correlates of response to anti-PD-1 immunotherapy in glioblastoma. *Nat Med* 2019;25:462–9.
- Sukumar M, Roychoudhuri R, Restifo NP. Nutrient competition: a new axis of tumor immunosuppression. *Cell* 2015;162:1206–8.
- Xia L, Oyang L, Lin J, et al. The cancer metabolic reprogramming and immune response. *Mol Cancer* 2021;20:28.
- Ryan DG, Murphy MP, Frezza C, et al. Coupling Krebs cycle metabolites to signalling in immunity and cancer. *Nat Metab* 2019;1:16–33.
- Dodard W, Tata A, Erick TK, et al. Inflammation-Induced lactate leads to rapid loss of hepatic tissue-resident NK cells. *Cell Rep* 2020;32:107855.
- Brand A, Singer K, Koehl GE, et al. LDHA-Associated lactic acid production blunts tumor immunosurveillance by T and NK cells. *Cell Metab* 2016;24:657–71.
- Liu N, Luo J, Kuang D, et al. Lactate inhibits Atp6v0d2 expression in tumor-associated macrophages to promote HIF-2 α -mediated tumor progression. *J Clin Invest* 2019;129:631–46.
- Wanders D, Hobson K, Ji X. Methionine restriction and cancer biology. *Nutrients* 2020;12:684.
- Strekalova E, Malin D, Good DM, et al. Methionine deprivation induces a targetable vulnerability in triple-negative breast cancer cells by enhancing TRAIL receptor-2 expression. *Clin Cancer Res* 2015;21:2780–91.
- Hens JR, Sinha I, Perodin F, et al. Methionine-restricted diet inhibits growth of MCF10AT1-derived mammary tumors by increasing cell cycle inhibitors in athymic nude mice. *BMC Cancer* 2016;16:349.
- He X, Xu C. Immune checkpoint signaling and cancer immunotherapy. *Cell Res* 2020;30:660–9.
- Qin S, Xu L, Yi M, et al. Novel immune checkpoint targets: moving beyond PD-1 and CTLA-4. *Mol Cancer* 2019;18:155.
- Liu B, Song Y, Liu D. Recent development in clinical applications of PD-1 and PD-L1 antibodies for cancer immunotherapy. *J Hematol Oncol* 2017;10:174.
- Yuan L, Tatineni J, Mahoney KM, et al. Vista: a mediator of quiescence and a promising target in cancer immunotherapy. *Trends Immunol* 2021;42:209–27.
- Huang X, Zhang X, Li E, et al. Vista: an immune regulatory protein checking tumor and immune cells in cancer immunotherapy. *J Hematol Oncol* 2020;13:83.
- Kakavand H, Jackett LA, Menzies AM, et al. Negative immune checkpoint regulation by vista: a mechanism of acquired resistance to anti-PD-1 therapy in metastatic melanoma patients. *Mod Pathol* 2017;30:1666–76.
- Liu J, Yuan Y, Chen W, et al. Immune-checkpoint proteins vista and PD-1 nonredundantly regulate murine T-cell responses. *Proc Natl Acad Sci U S A* 2015;112:6682–7.
- Lim S-O, Li C-W, Xia W, et al. Deubiquitination and stabilization of PD-L1 by CSN5. *Cancer Cell* 2016;30:925–39.
- Deng J, Li J, Sarde A, et al. Hypoxia-Induced vista promotes the suppressive function of myeloid-derived suppressor cells in the tumor microenvironment. *Cancer Immunol Res* 2019;7:1079–90.
- Rosenbaum SR, Knecht M, Mollaei M, et al. FOXD3 regulates vista expression in melanoma. *Cell Rep* 2020;30:510–24.
- Chen H, Yao J, Bao R, et al. Cross-Talk of four types of RNA modification writers defines tumor microenvironment and pharmacogenomic landscape in colorectal cancer. *Mol Cancer* 2021;20:29.
- Tong J, Wang X, Liu Y, et al. Pooled CRISPR screening identifies m⁶A as a positive regulator of macrophage activation. *Sci Adv* 2021;7:eabd4742.
- Yin H, Zhang X, Yang P, et al. Rna m6a methylation orchestrates cancer growth and metastasis via macrophage reprogramming. *Nat Commun* 2021;12:1394.
- Dong L, Chen C, Zhang Y, et al. The loss of RNA N6-adenosine methyltransferase Mettl14 in tumor-associated macrophages promotes CD8⁺ T cell dysfunction and tumor growth. *Cancer Cell* 2021;39:945–57.
- Ma S, Yan J, Barr T, et al. The RNA m6a reader YTHDF2 controls NK cell antitumor and antiviral immunity. *J Exp Med* 2021;218:e20210279.
- Li N, Kang Y, Wang L, et al. Alkbh5 regulates anti-PD-1 therapy response by modulating lactate and suppressive immune cell accumulation in tumor microenvironment. *Proc Natl Acad Sci U S A* 2020;117:20159–70.